Organic & Biomolecular Chemistry

Accepted Manuscript

ROYAL SOCIETY OF CHEMISTRY

www.rsc.org/obc

Organic & Biomolecular Chemistry

Cite this: DOI: 10.1039/c0xx00000x

www.rsc.org/xxxxxx

ARTICLE TYPE

Theoretical study of ternary indole-cation-anion complexes

Jorge A. Carrazana-García,[1]* Enrique M. Cabaleiro Lago,[1] Alba Campo Cacharrón,[1] Jesús Rodríguez Otero[2]

Received (in XXX, XXX) Xth XXXXXXXXX 20XX, Accepted Xth XXXXXXXXX 20XX

DOI: 10.1039/b000000x

The simultaneous interactions of an anion and a cation with a π system have been investigated using MP2 and M06-2X theoretical calculations. Indole was chosen as a model π system for its relevance in biological environments. Two different orientations of the anion: interacting with the N-H and with the C-H groups of indole, have been considered. The four cations (Na^+, NH_4^+, $C(NH_2)_3^+$ and $N(CH_3)_4^+$) and the four anions (Cl^-, NO_3^-, $HCOO^-$ and BF_4^-) included in the study are of biological interest. The total interaction energy of the ternary complexes has been calculated and separated in its two- and three-body components and all of them are further divided into their electrostatic, exchange, repulsion, polarization and dispersion contributions using the Local Molecular Orbital-Energy Decomposition Analysis (LMO-EDA) methodology. The binding energy of the indole-cation-anion complexes depends on both ions, with the cation having the strongest effect. The intense cation-anion attraction determines the geometric and energetic features in all ternary complexes. These structures, with both ions in the same side of the π system, show an anti-cooperative interaction. However, the interaction is not only determined by electrostatics, but also the polarization contribution is important. Specific interactions like the one established between the anion and the N–H group of indole or the proton transfer between an acidic cation and a basic anion play a significant role in the energetics and the structure of particular complexes. The presence of the polar solvent as modelled with the Polarizable Continuum Model (PCM) does not seem to have a significant effect in the geometry of the ternary complexes, but drastically weakens the interaction energy. Also, the strength of the interaction is reduced at a faster rate when the anion is pushed away, compared to the results obtained in gas phase. The combination of PCM with the addition of one water molecule indicates that the PCM method properly reproduces the main energetic and geometrical changes, even at quantitative level, but the explicit hydration allows refining the solvent effect and detecting cases that do not follow the general trend.

[1] *Departamento de Química Física, Facultade de Ciencias, Universidade de Santiago de Compostela. Campus de Lugo. Avenida Alfonso X El Sabio s/n, Lugo 27002, Lugo, SPAIN.*

[*] *Phone: +34982824132; e-mail: jorge.carrazana@usc.es*

[2] Centro de investigación en Química Biolóxica e Materiais Moleculares, CIQUS, Universidade de Santiago de Compostela, Rúa Jenaro de la Fuente s/n, Santiago de Compostela, 15782, (Spain)

† Electronic Supplementary Information (ESI) available: Results of the complete inter-fragment interaction energy analysis, obtained by LMO-EDA. Sensitivity of the binding energy with respect to the nature of the anion and to the nature of the cation. Optimized structures of the indole-cation-anion complexes selected for this study.

Introduction

The formation of molecular complexes, through chemical and/or physical interactions, is at the basis of supramolecular chemistry in the biological field.[1] Inter and intramolecular interactions determine the structure and folding of proteins and nucleic acids and, in general, play an important role in chemical reactions. Aggregation of molecules to clusters and the formation of condensed phases are also governed by nonbonding interactions.[2-5] In molecular recognition, the specificity and efficiency of the process is achieved by a combination of weak molecular interactions of different nature.[6]

The interaction between a cation and an aromatic moiety is a common motif in biological systems, usually involving side chains of aromatic and cationic amino acids. A typical example of the presence of cation-π interaction in protein chemistry could be represented by the often-observed contacts between adjacent cations (e.g., Na^+ and K^+) or the cationic side chain of arginine and lysine with those of phenylalanine, tyrosine and tryptophan, which have aromatic groups.[7-14] Recently, it has been revealed that cation-π interactions also strongly contribute to underwater adhesion of mussel-foot proteins,[15] which lack negatively charged residues but have abundant aromatic and positively charged groups. The adhesion mechanism discovered in these proteins provides important insight into the design and development of functional biomaterials and coatings that simulate the mussel cuticle coating. The important role of cation-π interaction in Chemistry, Biology, Materials Science, and nanosystems have been reviewed in recent publications.[2, 4, 5]

Significant experimental and theoretical work has been carried out to understand the cation-π interactions, their physical origin and mechanism. Computational Chemistry has shown that these interactions are not only of electrostatic nature, as suggested in previous studies.[16-18] Besides, in actual systems, cation-π interactions usually occur in conjunction with other non-bonding interactions. Therefore it is important to consider model structures in which multiple interactions occur together.[19-21] The effect of anions on the cation-π interactions is a matter of interest in the binding of biomolecules[22] and in the self-assembling of supramolecular structures.[23] Some investigations have considered the effect of the counter-ion upon the cation-π interaction in order to have a better understanding of these non-bonding interactions.[22, 24-28] However, most of these studies use fixed orientations and simplified aromatic structures together with the simplest, monoatomic ions and only two works address the problem at the ab-initio level: the one by Kim[27] that study the interaction of benzene with halide anions and with alkali and ammonium cations, and our own work[26] with benzene, guanidinium and chloride.

The present study includes a wider variety of ions, most of them polyatomic, that model amino acid groups that participate in the cation-π and cation-π-anion interactions frequently found in proteins and in other real systems. The studied complexes include monoatomic ions as Na^+ and Cl^-, along with more complex fragments such as NH_4^+ (model of the cationic end of lysine), $C(NH_2)_3^+$ (arginine), $N(CH_3)_4^+$ (acetylcholine), $HCOO^-$ (glutamic and aspartic acids) and the polyatomic anions NO_3^- and BF_4^-. Indole, present in the aromatic side chain of tryptophan, is employed as a model of a π-system. This molecule includes in its structure the benzene ring (present in phenylalanine and tyrosine) and has additionally a pentagonal aromatic ring containing a N-H group, similar to that found in the imidazole ring of histidine. The presence of the two conjugated rings and the N-H group gives indole the possibility for interacting as donor or acceptor.[29, 30] Therefore, it can interact with ions of both charges, working as a good ion-pair receptor[31] and it has been recognized as the most frequent fragment in the cation-π interactions observed in protein systems.[32] Of all possible combinations, fragments have been arranged to interact with each other in the following ways: $M^+\cdots\pi$, being M^+ a monoatomic cation (Na^+), C-H$\cdots\pi$, N-H$\cdots\pi$, $\pi^+\cdots\pi$, C-H$\cdots X^-$ and N-H$\cdots X^-$, where X represents the anion. The aim of this variety of model structures is to attempt more general conclusions.

The final part of the present work is devoted to the study of the effect that the solvent exerts over the indole-cation-anion interaction. This is an interesting issue because in most real systems the supramolecular complexes are formed in solution. The work done in this field applies one of the two main methods available: the micro-solvation approach[4, 33-42] or the use of a continuum model.[43-45] Both approximations to the solvation problem have its own benefits and drawbacks so, if the size of the system allows it, the combination of both methods is also employed with the aim of model simultaneously the specific and the non-specific solute-solvent interactions.[46, 47] Some model indole-cation-anion complexes were selected to study solvent effects by applying the Polarizable Continuum Model and a combination of PCM with the explicit addition of water.

Computational Details

In the model cation-π-anion systems studied it is assumed that each trimer is formed from its three isolated fragments. The main hypothesis is that the trends and conclusions reached from the study of the ternary complexes with free fragments can be extrapolated to real systems in which some of the fragments used are parts of bigger and complicated structures, like proteins. The geometries of the indole-cation-anion complexes were optimized at the M06-2X/6-31+G* and MP2/6-31+G* levels of calculation. Frequency calculations at the M06-2X/6-31+G* level were subsequently performed to determine whether the geometry optimizations had successfully located minima. In systems in which more than one minimum was found, the more stable one was selected. When several minima of the same system have similar stabilities, the structure that better follows the geometric trends selected for this study was preferred (the selection criteria applied in these cases are explained below, in the *Analysis of the geometry* section). The supermolecule approach was used for the calculation of the BSSE-free interaction energies at the M06-2X/6-31+G* and MP2(full)/aug-cc-pVDZ//MP2/6-31+G* levels of calculation.[48, 49] Accordingly, the interaction energy results from subtracting the energies of the fragments that constitute the complex from its energy, all of them calculated using the geometry and the whole basis set of the cluster:

$$\mathrm{E_{int}} = E_{ij\ldots}(ij\ldots) - \sum_i E_i^{clus}(ij\ldots) \qquad (1)$$

where terms in parentheses indicate the basis set employed and superscripts the geometry used in the calculation. As the geometry of the fragments changes when the complex is formed,

an additional contribution, the deformation energy (E_{def}) describing this effect must be included. E_{def} is obtained as the energy difference between the fragments in the cluster geometry and in isolation, using for each fragment its own basis set:

$$E_{def} = \sum_i \left(E_i^{clus}(i) - E_i^{isol}(i) \right) \quad (2)$$

The binding energy results from adding these two contributions: $E_{bind} = E_{int} + E_{def}$. Binding energies were further corrected with the corresponding zero-point energies (ZPE) using the ZPE obtained at the M06-2X/6-31+G* level of calculation.

On the other hand, applying the same scheme as in equation 1 to the three possible combinations of two fragments, the two-body interactions, E_{int} (M-X), E_{int} (M-I) and E_{int} (I-X), can be obtained and by means of the usual equation applicable in many-body analysis,[10, 49] the three-body interaction:

$$E_{int}\,(Thr) = E_{int} - E_{int}\,(M\text{-}X) - E_{int}\,(M\text{-}I) - E_{int}\,(I\text{-}X) \quad (3)$$

can also be calculated. E_{int} (Thr), also called cooperativity or anti-cooperativity depending on its sign,[10, 19, 50, 51] expresses the non-additive term of the interactions in the ternary IMX complexes.

The Polarizable Continuum Model (PCM) was used for modeling the effect of different solvents on the interactions. Two PCM models: C-PCM (in water) and IEF-PCM (in other solvents) were used for the optimization of the geometries and for the subsequent calculation of the energies, using always the M06-2X/6-31+G* level of theory. As previously advised,[52-54] the BSSE calculated at the same level of calculation in the gas phase with the re-optimized geometries in the solvent is added to the interaction energies obtained with PCM. All the previous calculations were done with the Gaussian09 suite of programs.[55]

For gaining understanding in the physical nature of the interactions, the different contributions to the interaction energies were obtained by using the Local Molecular Orbital Energy decomposition Analysis (LMO-EDA) method developed by Su and Li[56] as implemented in GAMESS.[57, 58] The interaction energy is decomposed in its electrostatic, exchange, repulsion and polarization contributions for every ternary complex and all of its possible pairs. The difference between the total interaction energy and the sum of all the previous contributions is computed and reported as the *dispersion* contribution[56] (even when with post-HF method in fact it corresponds to the contribution of the correlation energy).

Results and Discussion

Analysis of the geometry of the trimers.

Figure 1 shows the optimized structures for the complexes studied in this work as obtained at the M06-2X/6-31+G* level of calculation. In all ternary complexes (IMX) the anion interacts with the acidic hydrogen atoms of indole, forming simultaneously an ion pair with the cation, which is oriented towards the negatively charged aromatic electron cloud of indole. All complexes have both, M and X, in the same side of the indole molecule, as a consequence of the dominant role of ion pairing on the energetics of these systems, as already pointed out in previous work.[26] When the anion is placed in the "z" orientation (see Fig. 1), the anions favorably interact by means of a hydrogen bond interaction with the N-H group of indole. On the contrary, when the anion is placed opposite the N-H group, the "b" side, there are a number of possible configurations with similar stabilities, with the anion interacting with different C-H groups of indole. In these cases, the geometry with the anion located between the hexagonal and the pentagonal rings of indole, present in all IMXb complexes, was selected for the analysis with the purpose of maintaining a more coherent trend.

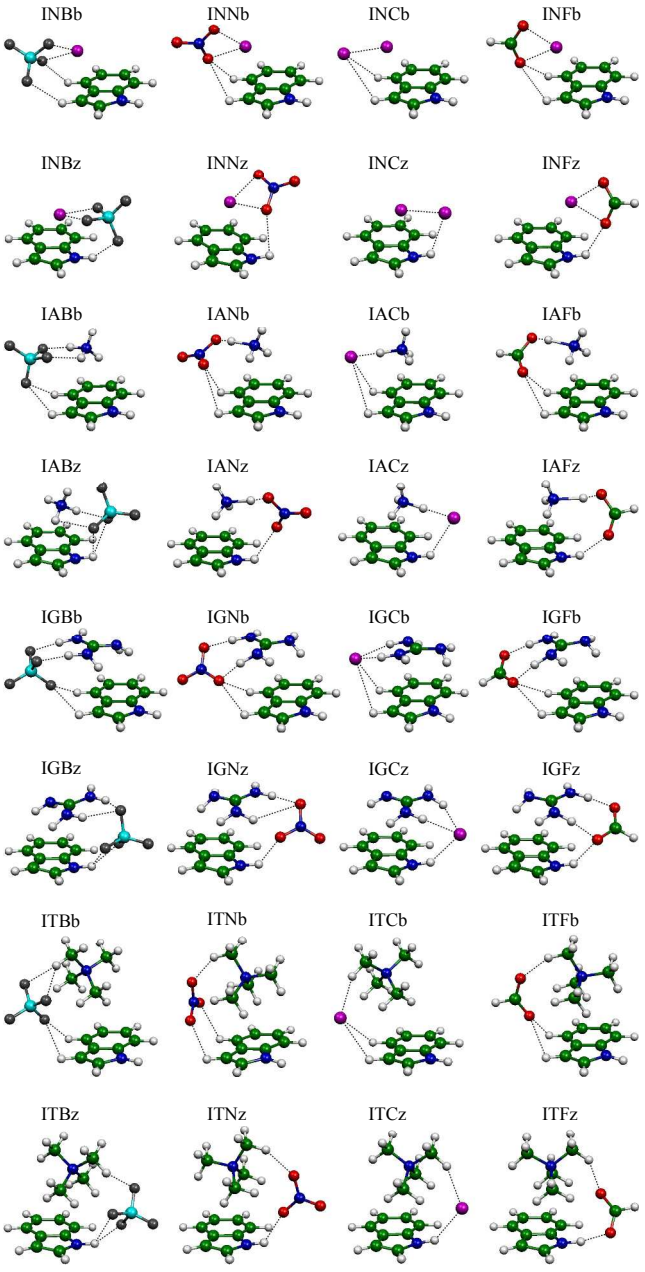

Fig. 1. Geometries optimized in gas phase at the M06-2X/6-31+G* level of calculation of the indole-cation-anion ternary complexes studied. The labels use the following acronyms: π-system: I = indole; Cation: N = Na^+, A = NH_4^+, G = $C(NH_2)_3^+$, T = $N(CH_3)_4^+$; Anion: B = BF_4^-, C = Cl^-, F = $HCOO^-$, N = NO_3^-; Orientation: z = anion by the side of the N-H group of indole, b = anion by the opposite side of the N-H group of indole. Dotted lines are visual guides.

In cases in which minima with multiple anion/cation orientations were found, only one of them was chosen, following stability and geometric criteria. As a result, eight different minima have been

selected for each of the studied cations, corresponding to a pair of structures for any given anion located by the "z" or "b" side of indole.

The transformation between the two kind of conformers was analyzed in the indole-ammonium-chloride complexes, observing that it is reached by rotating the ionic pair so that the cation adjust its position over the indole molecule while the anion moves around the pentagonal ring of indole between its positions in the minimums IACz and IACb.

Table 1. Total interaction energy (E_{int}), binding energy (E_{bind} = E_{int} + deformation energies) and E_{bind} + zero-point energy for the indole-cation-anion complexes studied in gas phase. M06-2X/6-31+G* results *in italics*, MP2(full)/aug-cc-pVDZ//MP2/6-31+G* results in plain text. All the values are in kcal/mol.

	E_{int}	E_{bind}	E_{bind} +ZPE[b]	E_{int}	E_{bind}	E_{bind}+ZPE[b]
	"z" orientation[a]			"b" orientation[a]		
INB	*-147.39*	*-144.68*	*-142.56*	*-140.78*	*-137.94*	*-136.09*
	-138.03	-133.01	-130.89	-133.65[c]	-129.85[c]	-128.00[c]
INN	*-152.43*	*-149.95*	*-148.07*	*-147.09*	*-145.53*	*-143.56*
	-145.18	-143.13	-141.25	-140.06[c]	-137.46[c]	-135.49[c]
INC	*-152.01*	*-150.83*	*-150.22*	*-145.65*	*-145.51*	*-144.22*
	-145.27	-144.06	-143.45	-138.76	-138.64	-137.35
INF	*-165.73*	*-163.51*	*-160.89*	*-160.22*	*-158.85*	*-156.22*
	-157.16	-155.37	-152.74	-151.60	-150.55	-147.92
IAB	*-134.23*	*-130.90*	*-127.94*	*-127.52*	*-124.26*	*-121.82*
	-132.10	-129.38	-126.43	-125.39	-122.22	-119.78
IAN	*-189.76*	*-139.40*	*-138.31*	*-194.72*	*-136.80*	*-135.72*
	-203.93	-138.22	-137.14	-207.94	-135.76	-134.68
IAC	*-150.34*	*-143.75*	*-143.27*	*-148.98*	*-136.71*	*-137.39*
	-145.99	-141.99	-141.51	-141.41	-134.73	-135.41
IAF	*-230.83*	*-161.04*	*-158.74*	*-228.48*	*-155.82*	*-153.80*
	-234.23	-157.10	-154.80	-231.48	-152.02	-150.01
IGB	*-126.92*	*-121.11*	*-117.71*	*-117.95*	*-112.21*	*-109.66*
	-124.40	-119.50	-116.10	-115.99	-111.00	-108.45
IGN	*-133.04*	*-126.13*	*-123.26*	*-125.26*	*-117.94*	*-115.74*
	-131.47	-125.74	-122.88	-123.78	-117.89	-115.70
IGC	*-139.18*	*-132.20*	*-130.10*	*-127.75*	*-120.62*	*-119.52*
	-138.34	-131.98	-129.88	-126.18	-120.15	-119.04
IGF	*-149.52*	*-141.25*	*-138.06*	*-141.73*	*-132.41*	*-130.24*
	-146.52	-139.50	-136.31	-138.36	-130.96	-128.79
ITB	*-106.63*	*-104.79*	*-102.56*	*-98.15*	*-96.83*	*-94.86*
	-104.66	-102.99	-100.76	-96.42	-95.11	-93.14
ITN	*-110.53*	*-108.42*	*-106.33*	*-102.15*	*-101.15*	*-99.10*
	-111.79	-110.78	-108.68	-101.51	-100.59	-98.53
ITC	*-116.44*	*-115.09*	*-113.45*	*-105.76*	*-105.10*	*-104.29*
	-115.99	-114.26	-112.61	-104.73	-103.95	-103.13
ITF	*-123.66*	*-121.32*	*-118.50*	*-112.75*	*-110.92*	*-108.60*
	-121.81	-119.82	-117.00	-109.85	-108.17	-105.85

(a) See Figure 1. (b) The E_{bind} of both of levels of calculation are corrected with the ZPE obtained at the M062X/6-31+G* level. (c) No MP2 minimum was found, the M06-2X/6-31+G* geometry was used in the calculations.

Comparing the binary complexes[39, 59-62] with the corresponding ternary cation-π-anion complexes, the presence of the anion causes the expected modifications on the distance and mutual orientation between the cation and the indole molecule. The most drastic change occurs in the complexes with the guanidinium cation. In binary complexes in gas phase, indole and guanidinium form a T-shaped complex,[26, 34, 39, 60, 63, 64] but in all the IGX complexes studied guanidinium and indole are in a parallel stacked orientation. Conformational searches in the Protein Data Bank for the interactions between the arginine side-chain and aromatic groups found that the frequency of the stacked geometry doubles the frequency of the T-shaped interaction (the ratio increases to about 7:2 when the aromatic group considered is the indole group of tryptophan).[65] So, when the N-H···π interaction, the most favorable in gas phase, competes with other interactions (with the anion or solvent molecules)[26, 34, 39, 60, 63, 64] the geometry changes to stacked, maximizing the cation-π contact area. This observation is important and potentially useful for protein docking studies due to the relevance of cation–π interactions involving arginine.

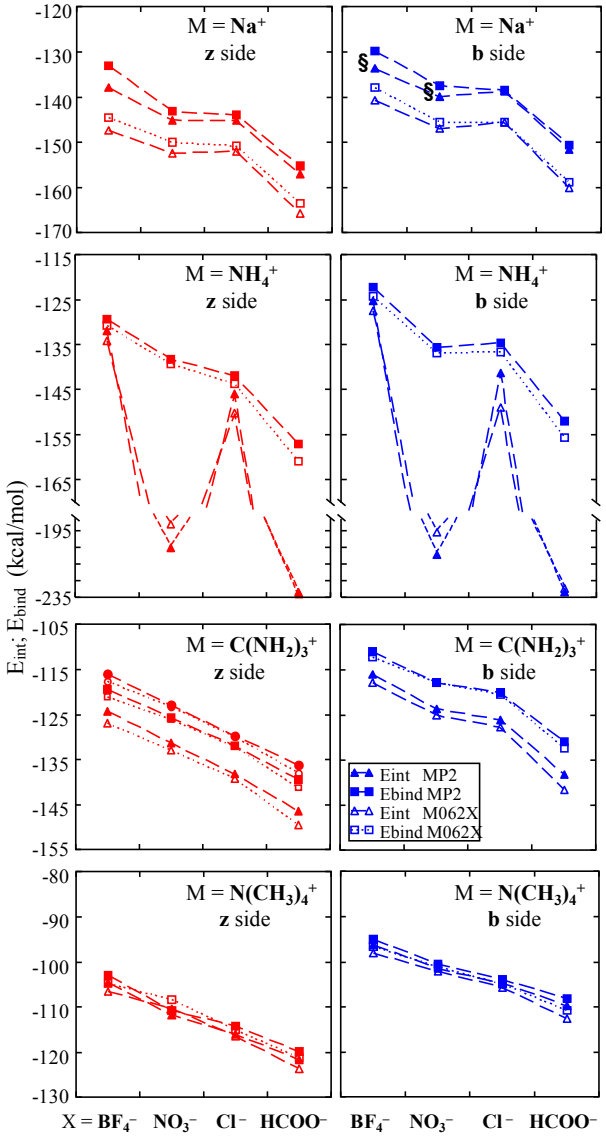

Fig. 2. Total interaction energy and binding energy for the indole-cation-anion complexes studied in gas phase (see Table 1). In the legend, common to the eight plots, empty symbols corresponds to the M06-2X/6-31+G* and filled symbols corresponds to the MP2(full)/aug-cc-pVDZ//MP2/6-31+G* results. § In the cases of indole-Na^+-BF_4^- and indole-Na^+-NO_3^- by the "b" side the MP2 geometry was not found and the energies MP2(full)/aug-cc-pVDZ//M06-2X/6-31+G* are presented.

Interaction and Binding Energies.

Table 1 shows the values of the total interaction energies and their corrections using the corresponding deformation and zero-point energies calculated in gas phase for all of the IMX

complexes included in the present study. These results are plotted in Fig. 2. It is observed that the values obtained with MP2/aug-cc-pVDZ//MP2/6-31+G* and M06-2X/6-31+G* show the same trends, being the systems with M = Na^+ those exhibiting the largest differences. In all the other systems the numerical results calculated with the two levels of theory used differ in only 2,5% of E_{bind} or below.

Ammonium cation shows a particular behavior when paired with basic anions. In complexes with formate as well as with nitrate (IAFb, IAFz, IANb and IANz in Fig. 1) the N-H bond of NH_4^+, pointing towards the anion is stretched about 45% to 63% with respect to the values for the isolated cation, indicating that a proton transfer is taking place. In complexes with chloride anion the mentioned N-H bond of NH_4^+ is also stretched, but to a smaller extent: 12% in IACz and 19% in IACb.

Table 2. Decomposition of the total interaction energy (kcal/mol) calculated at the MP2(full)/aug-cc-pVDZ//MP2/6-31+G* level of calculation into its pair contributions: cation-anion (M-X), cation-indole (M-I), indole-anion (I-X) and three-body (Thr = non-additivity).

	M-X	M-I	I-X	Thr
INBz	-119.38	-21.31	-12.87	15.54
INBb[(a)]	-121.58	-24.39	-2.72	15.05
INNz	-128.39	-26.39	-5.65	15.25
INNb[(a)]	-129.17	-24.51	-2.17	15.78
INCz	-127.15	-20.85	-13.65	16.37
INCb	-127.24	-23.45	-3.83	15.76
INFz	-140.81	-15.91	-17.32	16.87
INFb	-141.07	-23.54	-3.34	16.35
IABz	-109.29	-20.76	-14.09	12.04
IABb	-111.33	-23.79	-1.34	11.06
IANz	-193.48	-18.23	-10.70	18.49
IANb	-200.25	-21.03	-1.32	14.65
IACz	-125.12	-18.49	-18.13	15.75
IACb	-130.42	-22.49	-1.74	13.25
IAFz	-220.81	-15.41	-19.05	21.04
IAFb	-225.01	-20.32	-1.82	15.66
IGBz	-98.85	-17.68	-15.58	7.71
IGBb	-101.19	-18.87	-2.94	7.01
IGNz	-109.24	-16.76	-14.95	9.48
IGNb	-110.50	-17.76	-3.20	7.69
IGCz	-112.61	-15.70	-20.85	10.82
IGCb	-114.47	-17.41	-1.81	7.51
IGFz	-124.06	-15.16	-19.02	11.72
IGFb	-126.33	-16.87	-4.39	9.23
ITBz	-84.76	-10.81	-15.69	6.60
ITBb	-86.68	-13.32	-1.56	5.14
ITNz	-87.87	-12.67	-18.54	7.29
ITNb	-88.49	-14.71	-3.64	5.33
ITCz	-94.06	-10.10	-20.73	8.90
ITCb	-94.67	-12.62	-3.55	6.10
ITFz	-92.66	-12.31	-24.84	8.01
ITFb	-98.95	-14.65	-2.69	6.44

(a) No MP2 minimum was found, the M06-2X/6-31+G* geometry was used in the calculations.

As observed in Fig. 2, for all the cations, E_{int}, E_{bind} and E_{bind}+ZPE follow the stability sequence $BF_4^- < NO_3^- < Cl^- < HCOO^-$ (comparing absolute values). Outstanding exceptions to this ordering are the IAN (ammonium with nitrate) and IAF (ammonium with formate) complexes, in which the transfer of one acidic proton from the ammonium cation to the basic anions is accompanied by highly negative interaction energies. However, the stability sequence is recovered when the corresponding deformation energies (E_{bind} and E_{bind}+ZPE) are added.

Deformation is only relevant in systems where the proton transfer (total or partial) takes place, with contributions over 26% of the corresponding E_{int}.

All the complexes with the same cation and anion present a stronger interaction when the anion is in the "z" orientation because of the extra stabilization conferred by the interaction between the anion X and the N-H group of indole, more acidic than the C-H groups that interact with X on the "b" side.

As the charge of the four cations is the same, in complexes with the same anion the binding energies are ordered following the inverse sequence of its ionic volumes: $Na^+ > NH_4^+ > C(NH_2)_3^+ > N(CH_3)_4^+$ (comparing the absolute values). The only exception to this regularity are the IAFz and IAFb complexes, with binding energies about 2 kcal/mol more intense (MP2 values in Table 1) than INFz and INFb, inverting the $Na^+ - NH_4^+$ stability sequence observed in all other cases. This could be related to the extent of the proton transfer in each of these complexes. The complex containing ammonium and formate, IAFz, is the strongest complex among the ones the studied in the present work.

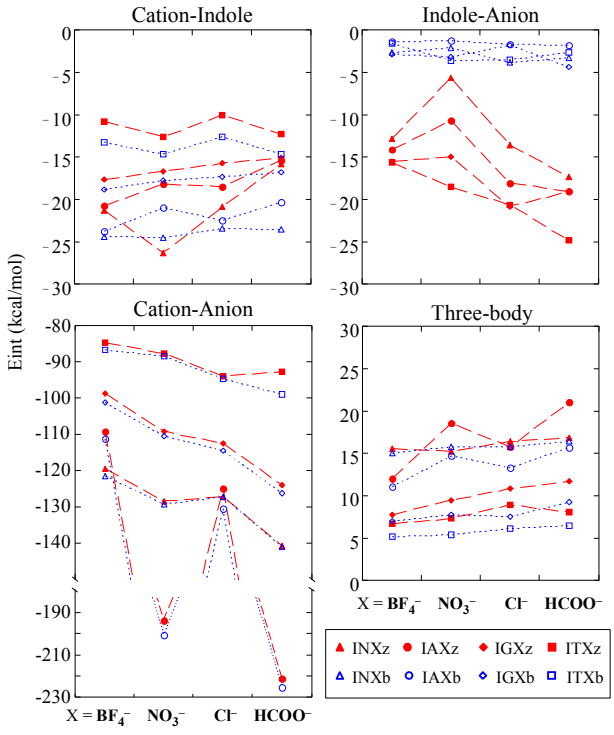

Fig. 3. Two- and three-body contributions to the interaction energy of the indole-cation-anion complexes studied (see Table 2).

Two and three-body contributions to E_{int}.

The interaction energy of the ternary IMX complexes can be decomposed into its two- and three-body contributions, with the results shown in Table 2 and Fig. 3. As expected, in all complexes the attraction between the cation and the anion represents by far the larger contribution to the interaction. The values of E_{int} (M-X) are clearly grouped by cation and, in general, follow the above-mentioned sequences for the anion and cation influence. Therefore, the interaction is weakest for tetramethyl-ammonium among cations and for BF_4^- among anions, and strongest in the subsets of sodium and formate complexes. In all

cases E_{int} (M-X) is slightly weaker (less negative) for the "z" complexes.

The stabilizing effect of the interaction between the anion and the N-H group of indole is emphasized in the plot of the indole-anion interaction in Fig. 3, where all the "b" complexes present E_{int} (I-X) around 5 to 20 kcal/mol less negative that the corresponding "z" complexes. It can be observed that in general, the I-X interaction is weaker for ternary complexes with the strongest M-X interaction. As the M-X interaction is greater the anion is forced to move away from the optimum geometry for the hydrogen bond with the N-H group of indole, resulting in weaker I-X interactions. Similarly, the weaker interaction of the anion with the C-H groups allows the cation to be located in a more favorable position for interacting with the indole molecule, leading to stronger interactions by the "b" side.

In most complexes the cation-π interaction is stronger than the indole-anion interaction, in many cases despite the stabilizing contribution of the N-H···X hydrogen bond in "z" complexes. However, in all the ITXz complexes the cation-π interaction contributes to the interaction less than the indole-anion interaction as a consequence of the large size of the tetramethylammonium cation. These observations underline the significant role of the cation in the stability of the ternary cation-π-anion complexes.

In all complexes E_{int} (Thr) is positive, showing that the non-additive contribution to the total interaction is anti-cooperative, as found before in other cation-π-anion complexes with the cation and the anion in the same side of the π-system.[26] As in the M-I interaction, the anion's nature has a limited impact on E_{int} (Thr). However, it can be observed that the three-body effect is more positive for ammonium and sodium cations (the most polarizing cations) whereas the smallest effects are observed in tetramethylammonium complexes. This is in agreement with the fact that in these systems non-additive effects mainly come from induction as will be confirmed below, and already suggested in a previous work.[26]

Table 3. NBO charge on cation (a.u.) calculated at the MP2(full)/aug-cc-pVDZ//MP2/6-31+G* level of calculation for the ternary complexes indole-cation-anion studied.

X =	BF_4^-	NO_3^-	Cl^-	$HCOO^-$
INXz	0.876	0.851	0.856	0.874
INXb	0.907[(a)]	0.869[(a)]	0.857	0.856
IAXz	0.906	0.625	0.773	0.605
IAXb	0.903	0.611	0.715	0.595
IGXz	0.894	0.848	0.837	0.815
IGXb	0.890	0.834	0.795	0.792
ITXz	0.935	0.917	0.892	0.913
ITXb	0.927	0.909	0.874	0.880

(a) No MP2 minimum was found, the M06-2X/6-31+G* geometry was used in the calculations.

Charge distribution.

Population analysis shows that indole is almost unchanged but a significant charge transfer exists between the anion and the cation. Table 3 shows the charge on the cations obtained from a Natural Bond Orbital analysis in all ternary complexes. As a rule, with any particular cation a minor influence of the anion is observed and the charge transfers are (mean values) between 0.086 a.u. in the ITXz group and 0.172 a.u. in the IGXb subset. With ammonium cation, IABb and IABz keep this trend, but the other IAX complexes do not. In the complexes IACz and IACb the cation loses 0.227 and 0.285 of its charge, respectively, reflecting the partial proton transfer commented above. More significant changes are observed in the complexes in which the cation is ammonium and the anion is formate or nitrate. In the cases of IANz, IANb, IAFz and IAFb, losses from 0.37 to 0.40 of the cation charge confirm that proton transfer has taken place.

Comparing the data in Tables 1 and 3 a relationship between the binding energy and the charge transfer arises. The correlation is not perfect but trends are clear within each subset of complexes of the same type. It can be observed that whereas tetramethylammonium shows the smallest charge transfers leading to the weakest complexes, sodium and ammonium exhibit large charge transfers in line with the greater stability of its complexes. These changes in the charge of cations and anions when forming the complexes can be extrapolated to proteins with similar aminoacids. The degree to which ions bind to the protein surface changes the effective charge of the protein counter-ions and the charge profile of the protein, with implications in the protein functionality and solubility.[66]

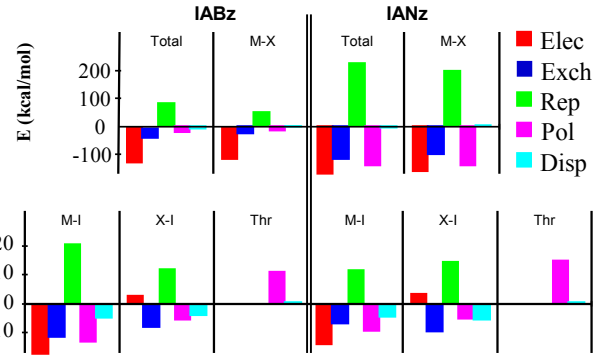

Fig. 4. Results of the LMO-EDA energy analysis (total interaction and its two- and three-body contributions) in two complexes: IABz shows the typical decomposition for the most of the cases studied and IANz corresponds to complexes in which exists proton transfer.

Energy Decomposition Analysis.

Table 4 shows results for the LMO-EDA decomposition of the trimer's interaction energies. Results for the two- and three-body interactions can be found in Tables SI-1 to SI-4, though two examples of the complete LMO-EDA decomposition are presented in Fig. 4. Most of the complexes studied show a similar pattern to the one presented by IABz in Fig. 4: the leading stabilizing force is electrostatic, mainly due to the cation-anion attraction, but polarization and dispersion make important contributions too. Polarization interaction contribution is significant in the total as well as in every two-body interaction and is essentially the unique component of the non-additive term. The importance of the dispersive contribution is larger as the volume of the fragments increases and when the stacked π^+-π interaction is present (IGX family, see Table 4).

The four systems in which the proton transfer can be considered almost complete (IAFb, IAFz, IANb and IANz) present a decomposition pattern similar to the one showed in Fig. 4 by the IANz complex. Since LMO-EDA is applied to the interaction energies (without the deformation energy correction) the displacement of the H^+ is reflected through abnormally large

polarization and repulsion components in the cation-anion and in the total interactions. The two-body and the three-body contributions behave similarly to the rest of the complexes considered above. The complexes IACz and IACb, in which the proton transfer can be considered partial, occupy an intermediate position between the two situations shown in Fig. 4.

Table 4. LMO-EDA results (in kcal/mol) for the total interaction in the indole-cation-anion complexes studied at the MP2(full)/aug-cc-pVDZ level of calculation.

	Elec	Exch	Rep	Pol	Disp
INBz	-159,18	-46,51	95,91	-25,09	-3,16
INBb[(a)]	-146,37	-23,82	52,26	-15,37	-0,35
INNz	-152,49	-24,54	51,91	-17,96	-2,10
INNb[(a)]	-155,56	-25,92	58,12	-16,70	0,01
INCz	-160,28	-32,66	68,55	-18,24	-2,64
INCb	-154,54	-25,53	57,89	-15,82	-0,76
INFz	-173,69	-30,85	64,12	-18,14	1,39
INFb	-166,13	-21,58	48,46	-15,23	2,88
IABz	-137,91	-48,70	90,84	-24,10	-12,23
IABb	-130,43	-43,72	81,45	-21,81	-10,89
IANz	-174,35	-113,78	219,84	-130,67	-4,98
IANb	-169,18	-116,30	222,11	-139,72	-4,85
IACz	-153,37	-70,66	130,67	-38,37	-14,27
IACb	-144,21	-67,69	126,75	-43,94	-12,33
IAFz	-192,76	-119,55	226,28	-154,62	6,42
IAFb	-183,44	-114,03	214,87	-156,12	7,23
IGBz	-130,76	-59,11	106,91	-23,29	-18,15
IGBb	-121,55	-51,31	92,62	-20,22	-15,52
IGNz	-139,24	-70,31	126,61	-28,75	-19,78
IGNb	-130,52	-65,93	118,91	-28,35	-17,89
IGCz	-149,86	-83,42	147,40	-30,80	-21,66
IGCb	-133,13	-75,17	131,85	-29,79	-19,95
IGFz	-162,06	-85,53	154,20	-36,33	-16,80
IGFb	-152,70	-80,24	145,86	-36,44	-14,85
ITBz	-106,66	-44,39	76,67	-14,44	-15,85
ITBb	-96,36	-39,82	67,47	-12,99	-14,72
ITNz	-114,18	-60,50	102,89	-18,17	-21,83
ITNb	-101,23	-54,82	91,87	-16,92	-20,41
ITCz	-125,15	-73,45	124,55	-22,80	-19,14
ITCb	-111,13	-63,43	106,23	-20,34	-16,06
ITFz	-130,48	-76,68	132,43	-29,52	-17,56
ITFb	-113,98	-61,60	103,26	-21,79	-15,73

(a) No MP2 minimum was found, the M06-2X/6-31+G* geometry was used in the calculations.

Fig. 5 focuses on the electrostatic and polarization contributions to the two-body interactions. As it can be seen in the lower plots, the electrostatic contribution leads the cation-anion interaction and the values are clearly grouped by cation family, being more intense as the radius of the cation decreases. For any particular cation, the effect of the anion sharply follows the above-mentioned series of intensity: BF_4^-< NO_3^- < Cl^- < $HCOO^-$. The only exceptions observed to these regularities are the cases with proton transfer. Cation-anion interactions dominate the properties of the ternary complexes under study and determine the trends observed in the total interaction (see Figs. 2 and 5). The polarization contribution to the cation-anion interaction is smaller than the electrostatic contribution but still significant, especially in the IGX group as well as in IAB, ITC and ITF complexes. The elongation of the N-H bond in the complexes with partial or extensive proton transfer is reflected in the abnormally intense polarization contribution observed in the ammonia complexes, except for IAB.

The middle plots of Fig. 5 show the electrostatic and polarization contributions to the indole-anion interaction. In the "b" complexes the electrostatic part of the I-X interaction is repulsive or almost zero (in IGBb and ITNb complexes). The polarization contribution to I-X interaction is about -5 kcal/mol for all the "b" complexes, and the nature of the anion or the cation has no influence on it. On the other hand, the "z" complexes have an extra-stabilization due to the interaction of the anion with the N-H group of the indole, which is reflected in an attractive electrostatic contribution, whose values are spread from -1.48 kcal/mol in INNz to -25.70 kcal/mol in ITFz, but in most of these complexes the values are grouped in the -10 to -20 kcal/mol interval. As expected, the polarization contribution to the I-X interaction is more attractive for the "z" than for the "b" complexes but without a definite trend for the anion or the cation nature.

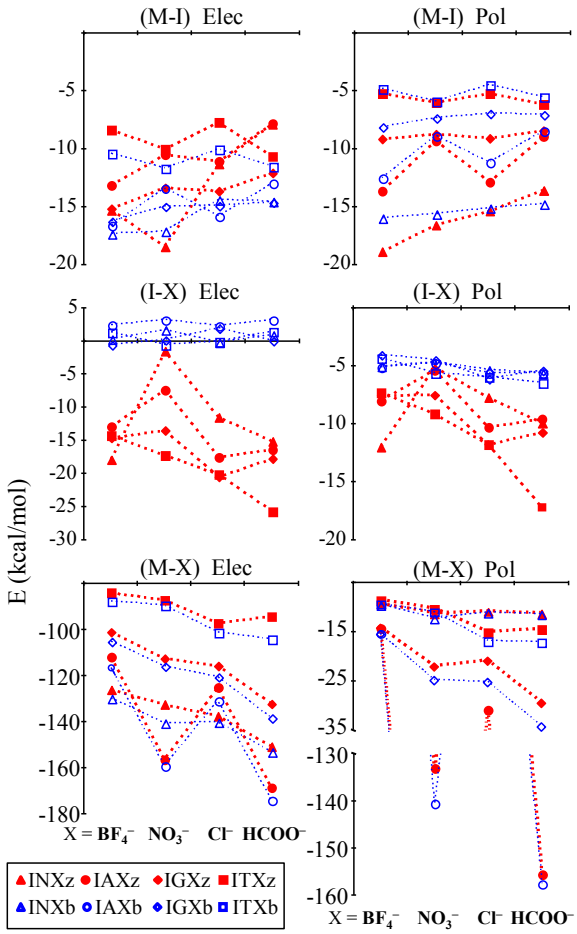

Fig. 5. Electrostatic and polarization contributions to the cation-indole (upper plots), indole-anion (middle plots) and cation-anion (lower plots) interactions present in all the indole-cation-anion complexes studied. The values plotted were calculated at the MP2/aug-cc-pVDZ level of calculation using the complete basis set of the corresponding ternary complex.

Finally, it is observed that the nature of the anion has a minor effect in the electrostatic and polarization contributions to the cation-indole interaction (upper plots in Fig. 5), but the orientation by which the anion is located has a systematic effect on these contributions. The "z" complexes exhibit less intense

electrostatic and slightly more intense polarization contribution to E_{int} (M-I). The polarization contributions to this interaction are again grouped following the polarizing effect of the cation.

The results obtained in the gas phase are important for discovering the factors controlling the interaction, but it is also important to consider the situations in which the complex is surrounded by solvent, since it deeply affects stabilities as shown in the following section.

Table 5. Total, two- and three-body interactions (in kcal/mol) for the indole-Na^+-Cl^- complexes calculated using the Polarizable Continuum Model for modeling media with different dielectric constant (ε) at the M06-2X/6-31+G* level of calculation. The geometries were re-optimized in the corresponding solvent before calculating the interactions.

	ε	Complex	M-X	M-I	I-X	Thr	Total
Gas Phase	*1.00*	**INCz**	-131.03	-20.65	-16.42	16.61	-151.48
		INCb	-138.68	-23.67	-1.70	14.11	-149.94
Toluene	*2.37*	**INCz**	-55.18	-9.55	-6.86	1.21	-70.39
		INCb	-56.73	-11.85	2.52	0.53	-65.52
1-Heptanol	*11.32*	**INCz**	-17.41	-4.78	-3.05	-1.53	-26.76
		INCb	-17.75	-5.89	0.78	-0.89	-23.75
Acetone	*20.49*	**INCz**	-13.33	-4.38	-2.73	-1.46	-21.90
		INCb	-13.57	-5.29	0.25	-0.69	-19.30
Acetonitrile	*35.69*	**INCz**	-11.22	-4.17	-2.58	-1.38	-19.36
		INCb	-11.40	-4.98	-0.05	-0.58	-17.00
DMSO[(a)]	*46.83*	**INCz**	-10.55	-4.12	-2.53	-1.35	-18.56
		INCb	-10.71	-4.89	-0.16	-0.51	-16.27
Water	*78.36*	**INCz**	-9.77	-4.09	-2.55	-1.16	-17.58
		INCb	-9.90	-4.83	-0.43	-0.30	-15.45

(a) DMSO = dimethyl-sulfoxide.

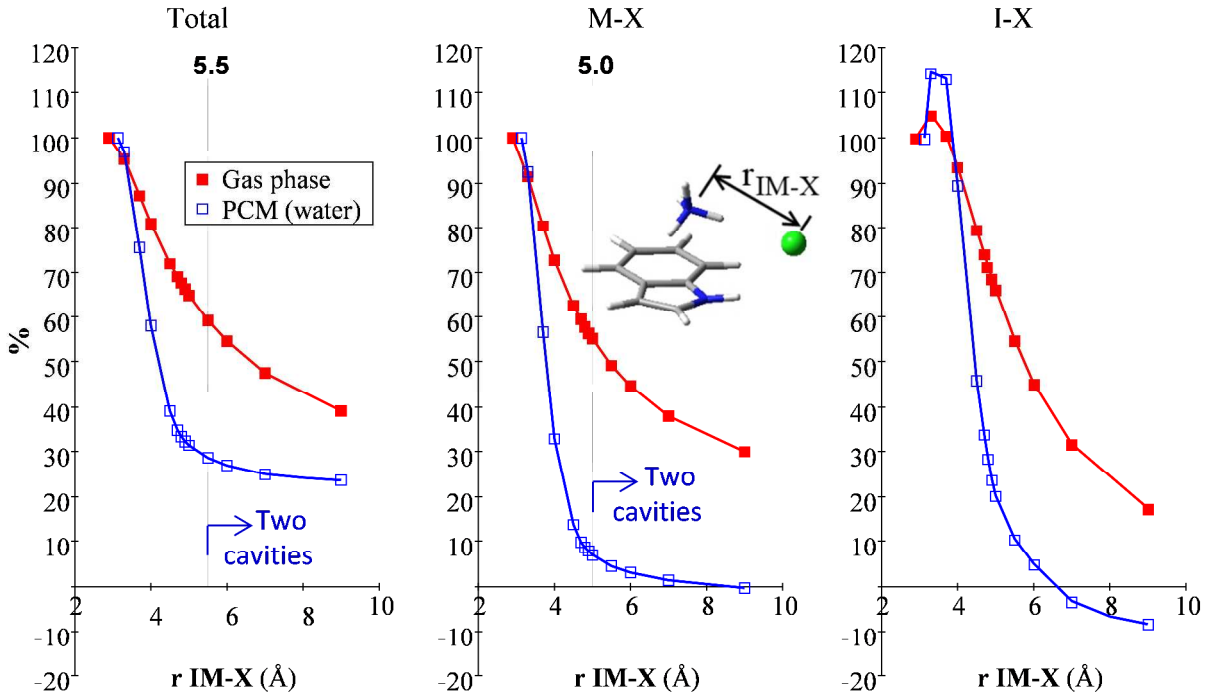

Fig. 6. Comparison of the results of the calculations at the M06-2X/6-31+G* level in the gas phase with the results at the same level in water (PCM) for the IACz complex as the anion is separated from the cation-indole fragment. Total, cation-anion and indole-anion interactions are referred to the corresponding values in the minimum and expressed in per-cent. The IM-X distances that limit the definition of one or two cavities in the PCM calculations has been highlighted.

Solvent effect.

The geometries optimized with PCM are similar to the gas-phase ones, as observed in previous work on methylammonium-aromatic systems.[46] The only exception observed is INCz complex in water, in which the Na^+ cation moves in the direction of the bulk solvent when the gas phase geometry is re-optimized using PCM. Also, since a solvent with a high dielectric constant favors charge separation, proton transfer from ammonium to the basic anions is hindered in water even in complexes including the most basis anions..

Although the changes in the distances between the fragments of the ternary complexes are small, the effect of the solvent in the interaction energy is drastic, as observed in Table 5. In a solvent with a very low dielectric constant like toluene (ε = 2.37) the interaction energy is reduced to less than half of the value

obtained in gas phase. This decrease affects all pair contributions and the effect in the non-additivity is drastic: a clear anti-cooperative interaction in gas phase, changes to be nearly zero in toluene. A further increase in the dielectric constant of the solvent (heptanol, ε = 11.32) again reduces total and two-body interaction energies to less than half of the values calculated in toluene, and E_{int} (Thr) now corresponds to a cooperative interaction. This last effect is not large but the trend is conserved in all solvents with larger ε. The effect of the dielectric constant of the solvent quickly begins to level off and reaches values similar to those observed in water. When ε is as low as 20 to 35 (acetone and acetonitrile) all the interactions are almost stabilized in the values calculated when the solvent is water.

Table 5. Influence of the solvent on the geometry and binding energy of some indole-ammonium-anion complexes. The structures were optimized at the M06-2X/6-31+G* level of calculation in gas phase (G.P.) or PCM=water, and are minima in their respective PES. The complexes with a "w" in its label (the structures are in Fig. SI-1) contain one water molecule. r (N-H) is the length, in Å, of the ammonium's N-H bond directed to the anion. E'_{bind} is the binding energy, in kcal/mol, for:

Indole + (ammonium+n·water) + anion → complex·n water (n = 0, 1)

complex		r (N-H)	relative change	E'_{bind}	relative change
IACz	G.P.	1.149		-143.78	
IACz_p	PCM	1.055	-8.2%	-15.54	-89.2%
IACz_w1p	PCM	1.046	-9.0%	-16.64	-88.4%
IACz_w2p	PCM	1.037	-9.7%	-15.39	-89.3%
IACz_w3p	PCM	1.045	-9.1%	-14.35	-90.0%
IACz_w4p	PCM	1.040	-9.5%	-16.62	-88.4%
IACz_w5p	PCM	1.042	-9.3%	-15.23	-89.4%
IACz_w6p	PCM	1.038	-9.7%	-16.84	-88.3%
IANz	G.P.	1.479		-139.42	
IANz_p	PCM	1.054	-28.7%	-16.93	-87.9%
IANz_w1p	PCM	1.047	-29.2%	-18.61	-86.7%
IANz_w2p	PCM	1.046	-29.3%	-17.69	-87.3%
IANz_w3p	PCM	1.048	-29.1%	-17.44	-87.5%
IAFz	G.P.	1.664		-161.07	
IAFz_p	PCM	1.547	-5.9%	-16.10	-90.0%
IAFz_w1p	PCM	1.450	-11.8%	-20.94	-87.0%
IAFz_w2p	PCM	1.052	-36.0%	-23.59	-85.4%
IAFz_w3p	PCM	1.442	-12.3%	-18.38	-88.6%

The effect of pulling away the anion maintaining the indole and the cation in its original positions is showed in Fig. 6 and Table SI-5. The starting geometries correspond to the structure of the IACz complex optimized in gas phase and in water, respectively. Fig. 6 shows E_{int} (Total), E_{int} (M-X) and E_{int} (I-X) relative to the value that each interaction has in the minimum obtained in gas phase and in water, respectively. It can be observed that the solvent damps the interactions very quickly and that E_{int} (Total) and E_{int} (M-X) in PCM change their trends at a distance of 5.5 Å in the first case and of 5.0 Å in the second. These IM–X distances coincide with the separation of the fragments above which the PCM algorithm defines independent cavities surrounding the solutes. The distance beyond which the cavity, initially unique, separates into two disjointed cavities and allows the existence of dielectric between the anion and the cation-π fragments, appears to be critical when calculating E_{int} (Total) and E_{int} (M-X). The effect is marginal for E_{int} (I-X), though it changes its sign in PCM as the distance increases, whereas in the gas phase E_{int} (I-X) is always negative and approaching to zero, as expected at long IM–X distances

The influence of the number of cavities on the calculated interactions and the trend of E_{int} (I-X) at long indole-anion distances are relevant issues and leave open the question about whether some of the observed effects are properties of the system or artifacts, resulting from the algorithm used by the PCM method.

A question arises as to whether PCM is capable of recovering possible specific effects due to the interaction of solvent molecules close to the complexes. In order to assess this point, PCM calculations have been performed in some model complexes including one explicit water molecule. Table 5 and Fig. SI-1 show the results obtained for indole-ammonium-anion complexes with anion = chloride, nitrate and formate. The main effect on the NH_4^+-X proton transfer and on the binding energy is caused by the continuum and the addition of a water molecule accounts for, proportionally, minor variations in E'_{bind} and in r (N-H). It is observed as well that the system IAFz_w2p, in which the water molecule behaves simultaneously as proton acceptor (from ammonium) and donor (to formate), deviates from the trend shown by its group. These results indicate that the PCM method properly reproduces the main trends, even at quantitative level, though the explicit hydration could allow detecting cases that do not follow the general trend. A detailed microhydration + PCM study is out of the scope of this work, but seems to be the best combination in order to improve our understanding of the cation-π-anion interactions in aqueous solution.

Conclusions

The different levels of calculation (MP2/aug-cc-pVDZ//MP2/6-31+G* and M06-2X/6-31+G*) employed to study the interaction of ternary cation-π-anion complexes perform similarly, showing comparable trends and numerical results.

All complexes exhibit large binding energies in gas phase as a consequence of the cation-anion interaction. The interaction of the anion with the N-H group of indole gives extra stabilization to the system and favors the complexes with the anion by this side of the molecule. Ammonium cation shows a particular behavior when paired with basic anions; a partial (when the anion is Cl^-) or almost complete (when the anion is NO_3^- or $HCOO^-$) proton transfer is observed. This proton transfer reflects in larger anion-cation charge transfer and abnormally high interaction energies. In general, the absolute value for the binding energy varies as expected from the chemical nature of the ions involved, following the sequences: $HCOO^- > Cl^- > NO_3^- > BF_4^-$ and $Na^+ > NH_4^+ > C(NH_2)_3^+ > N(CH_3)_4^+$. This ordering seems to follow the magnitude of the charge transferred between ions. The charge on indole remains almost unchanged but the anion transfers about 0.1 a.u. of the (negative) charge to the cation. The charge transfer is larger when the anion does not interact with the N-H of indole and can be up to 0.4 a.u. when proton transfer takes place.

It is observed that in the indole-cation-anion complexes studied E_{bind} is more sensitive to the cation nature than to the anion nature, especially when the anion does not interact directly with the N-H group of indole, reflecting the predominant role of the cation-π interaction over the indole-anion interaction in the ternary complexes. The decomposition of the total interaction in its two- and three-body contributions shows the predictable dominance of the cation-anion interaction. When the anion does

not interact with the N-H group of indole, the second contribution in importance is the cation-π interaction, but when the anion locates interacting with the N-H group, the indole-anion interaction contribution is almost of the same magnitude as the cation-π one. Since the cation and anion are in the same side of the π system, in all the complexes studied the three-body interaction is always anti-cooperative, decreasing the total interaction energy by 6-11%, being less important when less polarizing cations participate. Attending to the physical nature of the contributions to E_{int}, the LMO-EDA analysis revealed the expected dominance of the electrostatic contribution, even though polarization is very important too. Dispersion contribution is found to be important in the systems with big fragments and when the stacked π^{+}-π interaction is present.

The presence of a polar solvent does not seem to have a big effect on the geometry of most of the ternary complexes studied but drastically weakens the interaction. When the anion is pulled away, the interaction in water is damped very quickly in comparison with the results obtained in the gas phase. Specific solvent effects tested by including one explicit water molecule into the model lead to a similar global picture, though it allows identifying cases that may be out of the general rule obtained with the continuum model.

Acknowledgments

The authors thank to the Centro de Supercomputación de Galicia (CESGA) for the use of their computers.

References

1. H.-J. Schneider and A. Yatsimirski, *Principles and Methods in Supramolecular Chemistry*, Wiley, New York, 2000.
2. L. M. Salonen, M. Ellermann and F. Diederich, *Angew. Chem. Int. Ed.*, 2011, **50**, 4808-4842.
3. M. Nishio, *Phys. Chem. Chem. Phys.*, 2011, **13**, 13873-13900.
4. A. S. Mahadevi and G. N. Sastry, *Chem. Rev.*, 2012, **113**, 2100-2138.
5. D. A. Dougherty, *Acc. Chem. Res.*, 2012, **46**, 885-893.
6. N. J. Singh, H. M. Lee, I.-C. Hwang and K. S. Kim, *Supramol. Chem.*, 2007, **19**, 321-332.
7. G. Waksman, D. Kominos, S. C. Robertson, N. Pant, D. Baltimore, R. B. Birge, D. Cowburn, H. Hanafusa, B. J. Mayer, M. Overduin, M. D. Resh, C. B. Rios, L. Silverman and J. Kuriyan, *Nature*, 1992, **358**, 646-653.
8. P. C. Kearney, L. S. Mizoue, R. A. Kumpf, J. E. Forman, A. McCurdy and D. A. Dougherty, *J. Am. Chem. Soc.*, 1993, **115**, 9907-9919.
9. S. Mecozzi, A. P. West and D. A. Dougherty, *J. Am. Chem. Soc.*, 1996, **118**, 2307-2308.
10. M. J. Elrod and R. J. Saykally, *Chem. Rev.*, 1994, **94**, 1975-1997.
11. J. P. Gallivan and D. A. Dougherty, *J. Am. Chem. Soc.*, 2000, **122**, 870-874.
12. N. Zacharias and D. A. Dougherty, *Trends Pharmacol. Sci.*, 2002, **23**, 281-287.
13. R. Wu and T. B. McMahon, *J. Am. Chem. Soc.*, 2008, **130**, 12554-12555.
14. L. M. Salonen, C. Bucher, D. W. Banner, W. Haap, J.-L. Mary, J. Benz, O. Kuster, P. Seiler, W. B. Schweizer and F. Diederich, *Angew. Chem. Int. Ed.*, 2009, **48**, 811-814.
15. Q. Lu, D. X. Oh, Y. Lee, Y. Jho, D. S. Hwang and H. Zeng, *Angew. Chem. Int. Ed.*, 2013, **52**, 3944-3948.
16. T. J. Shepodd, M. A. Petti and D. A. Dougherty, *J. Am. Chem. Soc.*, 1988, **110**, 1983-1985.
17. M. Albertí, A. Aguilar, J. M. Lucas and F. Pirani, *J. Phys. Chem. A*, 2010, **114**, 11964-11970.
18. J. A. Carrazana-García, J. s. Rodríguez-Otero and E. M. Cabaleiro-Lago, *J. Phys. Chem. B*, 2011, **115**, 2774-2782.
19. D. Vijay and G. N. Sastry, *Chem. Phys. Lett.*, 2010, **485**, 235-242.
20. I. Alkorta, F. Blanco, P. Deyà, J. Elguero, C. Estarellas, A. Frontera and D. Quiñonero, *Theor. Chem. Acc.*, 2010, **126**, 1-14.
21. A. Ebrahimi, S. M. Habibi Khorassani, R. Behazin, S. Rezazadeh, A. Azizi and P. Karimi, *Mol. Phys.*, 2013, **112**, 41-48.
22. S. Bartoli and S. Roelens, *J. Am. Chem. Soc.*, 2002, **124**, 8307-8315.
23. T. B. Gasa, C. Valente and J. F. Stoddart, *Chem. Soc. Rev.*, 2011, **40**, 57-78.
24. M. Albertí, A. Aguilar and F. Pirani, *J. Phys. Chem. A*, 2009, **113**, 14741-14748.
25. S. Bartoli and S. Roelens, *J. Am. Chem. Soc.*, 1999, **121**, 11908-11909.
26. J. A. Carrazana-García, J. Rodríguez-Otero and E. M. Cabaleiro-Lago, *J. Phys. Chem. B*, 2012, **116**, 5860-5871.
27. D. Kim, E. C. Lee, K. S. Kim and P. Tarakeshwar, *J. Phys. Chem. A*, 2007, **111**, 7980-7986.
28. P.-O. Norrby and T. Liljefors, *J. Am. Chem. Soc.*, 1999, **121**, 2303-2306.
29. E. M. Cabaleiro-Lago, J. Rodriguez-Otero and A. Pena-Gallego, *J. Chem. Phys.*, 2011, **135**, 134310/1-134310/8.
30. T. v. Mourik, S. L. Price and D. C. Clary, *Chem. Phys. Lett.*, 2000, **331**, 253-261.
31. K. N. Skala, K. G. Perkins, A. Ali, R. Kutlik, A. M. Summitt, S. Swamy-Mruthinti, F. A. Khan and M. Fujita, *Tetrahedron Lett.*, 2010, **51**, 6516-6520.
32. J. P. Gallivan and D. A. Dougherty, *Proc. Natl. Acad. Sci. USA*, 1999, **96**, 9459-9464.
33. A. S. Reddy, H. Zipse and G. N. Sastry, *J. Phys. Chem. B*, 2007, **111**, 11546-11553.
34. N. J. Singh, S. K. Min, D. Y. Kim and K. S. Kim, *J. Chem. Theory Comput.*, 2009, **5**, 515-529.
35. H. M. Lee, P. Tarakeshwar, J. Park, M. R. Kołaski, Y. J. Yoon, H.-B. Yi, W. Y. Kim and K. S. Kim, *J. Phys. Chem. A*, 2004, **108**, 2949-2958.
36. E. M. Cabaleiro-Lago, J. Rodríguez-Otero and Á. Peña-Gallego, *J. Chem. Phys.*, 2011, **135**, 214301/1-214301/9.
37. A. Campo-Cacharron, E. M. Cabaleiro-Lago and J. Rodriguez-Otero, *ChemPhysChem*, 2012, **13**, 570-577.
38. A. Campo-Cacharrón, E. M. Cabaleiro-Lago and J. Rodríguez-Otero, *Theor. Chem. Acc.*, 2012, **131**, 1290-1213.
39. A. Rodríguez-Sanz, E. Cabaleiro-Lago and J. Rodríguez-Otero, *J. Mol. Model.*, 2014, **20**, 1-10.
40. A. a. Rodríguez-Sanz, E. M. Cabaleiro-Lago and J. Rodríguez-Otero, *Org. Biomol. Chem.*, 2014, 2938-2949.
41. A. A. Rodriguez-Sanz, J. Carrazana-Garcia, E. M. Cabaleiro-Lago and J. Rodriguez-Otero, *J. Mol. Model.*, 2013, **19**, 1985-1994.
42. J. S. Rao, H. Zipse and G. N. Sastry, *J. Phys. Chem. B*, 2009, **113**, 7225-7236.
43. J. Tomasi and M. Persico, *Chem. Rev.*, 1994, **94**, 2027-2094.
44. C. J. Cramer and D. G. Truhlar, *Chem. Rev.*, 1999, **99**, 2161-2200.
45. J. Tomasi, B. Mennucci and R. Cammi, *Chem. Rev.*, 2005, **105**, 2999-3094.
46. C. Adamo, G. Berthier and R. Savinelli, *Theor. Chem. Acc.*, 2004, **111**, 176-181.
47. S. Thicoipe, P. Carbonniere and C. Pouchan, *Phys. Chem. Chem. Phys.*, 2013, **15**, 11646-11652.
48. S. F. Boys and F. Bernardi, *Mol. Phys.*, 1970, **18**, 553-556.
49. G. Chałasiński and M. M. Szczęśniak, *Chem. Rev.*, 2000, **100**, 4227-4252.
50. A. Frontera, D. Quinonero, A. Costa, P. Ballester and P. M. Deya, *New J. Chem.*, 2007, **31**, 556-560.
51. D. Vijay, H. Zipse and G. N. Sastry, *J. Phys. Chem. B*, 2008, **112**, 8863-8867.
52. J. M. Hermida-Ramon, M. Sanchez-Lozano and C. M. Estevez, *Phys. Chem. Chem. Phys.*, 2014, **16**, 6108-6117.
53. M. Sanchez-Lozano, N. Otero, J. M. Hermida-Ramon, C. M. Estevez and M. Mandado, *J. Phys. Chem. A*, 2011, **115**, 2016-2025.
54. A. Zawada, R. W. Góra, M. M. Mikołajczyk and W. Bartkowiak, *J. Phys. Chem. A*, 2012, **116**, 4409-4416.

55. M. J. Frisch, G. W. Trucks, H. B. Schlegel, G. E. Scuseria, M. A. Robb, J. R. Cheeseman, G. Scalmani, V. Barone, B. Mennucci, G. A. Petersson, H. Nakatsuji, M. Caricato, X. Li, H. P. Hratchian, A. F. Izmaylov, J. Bloino, G. Zheng, J. L. Sonnenberg, M. Hada, M. Ehara, K. Toyota, R. Fukuda, J. Hasegawa, M. Ishida, T. Nakajima, Y. Honda, O. Kitao, H. Nakai, T. Vreven, J. J. A. Montgomery, J. E. Peralta, F. Ogliaro, M. Bearpark, J. J. Heyd, E. Brothers, K. N. Kudin, V. N. Staroverov, R. Kobayashi, J. Normand, K. Raghavachari, A. Rendell, J. C. Burant, S. S. Iyengar, J. Tomasi, M. Cossi, N. Rega, J. M. Millam, M. Klene, J. E. Knox, J. B. Cross, V. Bakken, C. Adamo, J. Jaramillo, R. Gomperts, R. E. Stratmann, O. Yazyev, A. J. Austin, R. Cammi, C. Pomelli, J. W. Ochterski, R. L. Martin, K. Morokuma, V. G. Zakrzewski, G. A. Voth, P. Salvador, J. J. Dannenberg, S. Dapprich, A. D. Daniels, Ö. Farkas, J. B. Foresman, J. V. Ortiz, J. Cioslowski and D. J. Fox, *Gaussian 09*, 2009.
56. P. Su and H. Li, *J. Chem. Phys.*, 2009, **131**, 014102/1-014102/16.
57. M. W. Schmidt, K. K. Baldridge, J. A. Boatz, S. T. Elbert, M. S. Gordon, J. H. Jensen, S. Koseki, N. Matsunaga, K. A. Nguyen, S. Su, T. L. Windus, M. Dupuis and J. A. Montgomery, *J. Comput. Chem.*, 1993, **14**, 1347-1363.
58. M. S. S. Gordon, M. W. , in *Theory and Applications of Computational Chemistry*, ed. G. F. Clifford E. Dykstra, Kwang S. Kim, Gustavo E. Scuseria, Elsevier, Amsterdam, 2005.
59. C. Ruan, Z. Yang, N. Hallowita and M. T. Rodgers, *J. Phys. Chem. A*, 2005, **109**, 11539-11550.
60. F. Blanco, B. Kelly, I. Alkorta, I. Rozas and J. Elguero, *Chem. Phys. Lett.*, 2011, **511**, 129-134.
61. Z.-X. Wang, J.-C. Zhang and W.-L. Cao, *Chin. J. Chem* . 2006, **24**, 1523-1530.
62. T. Liu, W. Zhu, J. Gu, J. Shen, X. Luo, G. Chen, C. M. Puah, I. Silman, K. Chen, J. L. Sussman and H. Jiang, *J. Phys. Chem. A*, 2004, **108**, 9400-9405.
63. R. Sedlak, K. E. Riley, J. Rezac, M. Pitonak and P. Hobza, *ChemPhysChem*, 2013, **14**, 698-707.
64. S. Kozuch and J. M. L. Martin, *J. Chem. Theory Comput.*, 2013, **9**, 1918-1931.
65. P. B. Crowley and A. Golovin, *Proteins: Structure, Function, and Bioinformatics*, 2005, **59**, 231-239.
66. P. E. Mason, C. E. Dempsey, L. Vrbka, J. Heyda, J. W. Brady and P. Jungwirth, *J. Phys. Chem. B*, 2009, **113**, 3227-3234.